ISSN 1330-3651(Print), ISSN 1848-6339 (Online)
https://doi.org/10.17559/TV-20230918000947
Original scientific paper

Enhanced Lane Recognition for Automated Warning Sign Placement Using Canny Edge Detection

Yuan-shuai LAN*, Qian WANG, Jing-gui YANG, Xue-qin MENG, Yao YANG

Abstract: Real-time lane recognition is critical for intelligent roadside warning sign vehicles that provide post-accident precautions. However, lane interference, uneven lighting, and night time dimness can impair automatic cruise control. This paper presents an enhanced lane recognition methodology using Canny edge detection to enable automated placement of roadside warning signs. Image preprocessing via multi-directional Sobel filtering improves edge detection across varied lighting. Experiments demonstrated up to 85% lane recognition accuracy using the proposed techniques, outperforming prior thresholding approaches. An optimized PID controller enabled precise vehicle control based on lane data. The system was implemented on a K210 controller, validating real-time embedded performance. By overcoming lane detection deficiencies, this research enables reliable automated warning sign deployment to enhance road safety.

Keywords: canny filtering; dynamic lane recognition method; intelligent roadside warning sign vehicles; real-time lane recognition; Sobel edge detection

1 INTRODUCTION

Currently, with the development of smart automobiles and continuous improvement of road traffic, there is a growing demand for intelligent warning tripod [1, 2]. Lane detection is one of the important technologies for the safe operation of intelligent warning signs, and researchers have been focusing on this issue. Existing lane detection technologies have made significant progress to some extent, but there are still challenges in accuracy and stability under complex road conditions [3, 4]. Many lane detection technologies use traditional image processing, computer vision, and deep learning methods to identify lane lines on roads in various environmental conditions [5-7]. However, they still face some challenges in complex and uncertain road conditions. Especially in adverse weather conditions, such as rainy or snowy weather or heavy fog, traditional lane detection technologies often struggle to provide accurate identification results [8]. Furthermore, road markings may become blurred or damaged due to prolonged use, further increasing the difficulty of lane detection [9]. Therefore, this research aims to improve lane detection technology, especially in complex road conditions, with the goal of enhancing the performance of intelligent warning tripods while reducing hardware costs. To achieve this goal, we enhance edge information using the multi-directional Sobel operator and improve the Canny edge detection technique to enhance the reliability of lane detection, ensuring the normal operation of intelligent warning tripods in various road conditions.

2 LITERATURE SURVEY

Researchers mainly employ two mainstream approaches for lane detection: traditional image processing methods and deep learning-based methods.

Lane detection algorithms based on traditional image processing primarily identify lane regions through edge detection, filtering, and combine algorithms such as the Hough transform and RANSAC for lane detection. These methods require manual adjustment of filter operators and parameters tailored to specific street scene characteristics, leading to a significant workload and limited robustness.

[1] Lane detection based on the Hough transform is a widely used method in the field of computer vision [10-15]. This algorithm converts edge detection results from the image into Hough space to detect straight lines in the image. Each peak represents a straight line, allowing it to detect lanes of various angles and lengths. However, this method has poor performance in detecting curved lane lines, requires significant computational resources, and is sensitive to parameters. They applied the Hough transform to detected points to identify straight lines. Most of these algorithms were designed for lane detection in clear daytime conditions and may not be suitable for night time road lane detection.

[2] Lane detection based on LSD lines uses the Line Segment Detector (LSD) algorithm [16, 17]. It first identifies candidate endpoints of lines through multi-scale edge detection and then determines the position, direction, and length of the lines. This method is suitable for detecting both straight and curved lane lines, operates at a relatively fast speed, and exhibits some tolerance to noise. However, it is not suitable for detecting road features beyond lane lines.

[3] Lane detection based on a bird's-eye view transformation involves transforming the original image through a perspective transformation to project lane lines from the image to a top-down view, where straight or curved lines are detected [18, 19]. This method is suitable for detecting curved and differently sized lane lines, providing better lane shape estimation. However, it requires precise camera calibration and transformation matrices, is sensitive to changes in camera angle and pose, and may lose some surrounding environmental information.

[4] Fitting-based lane detection identifies lane feature points in the image and uses fitting techniques, such as polynomial fitting, to fit the shape of lane lines [20-22]. This method is suitable for various lane shapes, including curves, and can provide lane parameters such as curvature and direction. However, it is sensitive to noise and occlusions, requiring the selection of appropriate fitting models and parameters. It lacks robustness in cases of lane line discontinuity or absence.

[5] Lane detection based on parallel perspective vanishing points detects parallel lines in the image and finds their intersection, known as the parallel perspective vanishing point, to estimate the position of lane lines [23-25]. This method is suitable for detecting straight lane lines, relatively simple, requires no complex fitting or transformation, and has some tolerance to noise. However, it is not suitable for detecting curved lane lines, may lack accuracy in complex road structures, and is sensitive to changes in camera angle and pose.

Currently, deep learning-based lane detection algorithms, due to their high accuracy, have become the mainstream approach. Typically, the network structures for object detection are complex with a large number of parameters, which places high demands on computational capabilities and results in poor real-time performance. This is especially challenging for vehicle-mounted cameras with speed requirements for FPN, making them unsuitable for implementations based on K210.

[1] Lane detection based on semantic segmentation employs deep learning techniques to classify image pixels into lane line or background categories, achieving lane line segmentation [26-28]. In particular, SCNN [29] and SAD methods excel in detecting narrow lane lines and capturing lane details [30, 31]. However, these methods are limited by relatively slow processing speeds; for instance, SCNN operates at a frame rate of only 7.5 FPS, which may not be sufficiently fast for real-time applications. While SAD introduces an information distillation module to improve speed, performance remains constrained.

[2] Row-based classification methods employ an image grid partitioning strategy, dividing the image into rows and performing lane line detection in each row [32]. The model predicts the cell most likely to contain lane markings in each row to detect lane lines. Methods like E2E-LMD, IntRA-KD, and UFAST [33-38] demonstrate excellent detection speed, with UFAST even reaching up to 200 FPS, making it suitable for scenarios requiring fast real-time detection. However, as only one cell is chosen per row, it may miss certain lane line information.

[3] Anchor-based lane detection methods utilize object detection algorithms such as YOLOv5 and SSD [39-41] to detect lane lines. Some of the latest methods, like LaneATT [42], introduce anchor-based lane detection attention mechanisms. In addition to local information, it also emphasizes global information, such as processing in situations such as occlusion, missing or weak display. These methods excel in terms of speed and performance, with LaneATT even achieving a high frame rate of 250 FPS. However, these methods typically require a significant amount of annotated data and complex model training, necessitating more computational resources and time.

[4] Polynomial-based methods employ fitting the shape of lane lines, typically using polynomial functions to represent lane curvature [43-45]. In theory, this method can adapt to various lane shapes, including curves. However, actual performance may be limited by dataset constraints and the chosen fitting model, requiring a substantial amount of data for model training and potential parameter adjustments for different road types.

[5] The Fast Draw method combines segmentation and row classification techniques [46], eliminating the need for post-processing steps. However, it must overcome the limitations of both segmentation and row classification methods. On the other hand, the PolyLaneNet [47] method boasts faster speed but is affected by existing imbalanced datasets, potentially leading to biases.

Based on the research findings mentioned above, and considering the issues with traditional image processing and the high computational requirements of deep learning methods, this paper introduces an approach using an 8-direction Sobel operator to enhance edges, followed by the application of the Canny algorithm to extract lane lines. This method enhances the completeness of edge detection in various environments, exhibiting improved filtering and edge-preserving capabilities. Building upon this improved algorithm, the paper utilizes a K210 microcontroller as the main control unit to design and implement an intelligent visual warning sign. This system is designed to adapt to different environmental applications, and it demonstrates good functionality and performance, meeting the real-time hardware requirements for lane detection in intelligent warning signs.

3 RESEARCH METHOD

3.1 Basic Theory

[1] Laplacian operator. The Laplacian operator is an isotropic operator, and its template is shown in Fig. 1 [23]:

0	1	0
1	-4	1
0	1	0

Figure 1 Laplacian operator template

The Laplacian transformation of an image $f(x, y)$ is defined as shown in Eq. (1):

$$\nabla^2 f = \frac{\partial^2 f}{\partial x^2} + \frac{\partial^2 f}{\partial y^2} \tag{1}$$

Its discrete form is shown in Eq. (2):

$$\nabla^2 f = \begin{bmatrix} f(x+1, y) + (x-1, y) + \\ + f(x, y+1) + f(x, y-1) \end{bmatrix} - 4f(x, y) \tag{2}$$

[2] Sobel operator. The Sobel detection operator is an edge detection method based on gradient operators. It uses horizontal and vertical templates to convolve with the corresponding image data. It performs weighted calculations on discrete data [48]. Its definition is as follows:

$$\begin{aligned} \Delta G_x &= f(x-1, y+1) + 2f(x, y+1) + f(x+1, y+1) - \\ &- f(x-1, y-1) - 2f(x-1, y-1) - f(x-1, y-1) \\ \Delta G_y &= f(x-1, y-1) + 2f(x-1, y) + f(x-1, y+1) - \\ &- f(x+1, y-1) - 2f(x+1, y-1) - f(x+1, y+1) \\ G\left[f(x, y)\right] &= \left|\Delta G_x\right| + \left|\Delta G_y\right| \end{aligned} \tag{3}$$

Its horizontal and vertical templates are shown in Fig. 2:

1	2	1		1	0	-1
0	0	0		2	0	-2
-1	-2	-1		1	0	-1

Figure 2 Sobel operator templates

[3] Prewitt operator. The Prewitt operator convolves the image with horizontal and vertical convolution kernels separately for each pixel, and takes the maximum value between the two as the output value [49]. This gradient operator can be defined as:

$$\begin{aligned}
&\Delta G_x = f(x-1, y+1) + f(x, y+1) + f(x+1, y+1) - \\
&- f(x-1, y-1) - f(x, y-1) - f(x-1, y-1) \\
&\Delta G_y = f(x-1, y-1) + f(x-1, y) + f(x-1, y+1) - \\
&- f(x+1, y-1) - 2(x+1, y) - f(x+1, y+1) \\
&G(x, y) = \surd\left(\Delta G_x \wedge 2 + \Delta G_y \wedge 2\right)
\end{aligned} \tag{4}$$

Its template is shown in Fig. 3:

-1	-1	-1		-1	0	1
0	0	0		-1	0	1
1	1	1		-1	0	1

Figure 3 Prewitt operator template

3.2 Improved Lane Detection Algorithm

Image edges refer to areas in an image where pixel values undergo abrupt changes relative to their surroundings [50]. They effectively outline the contours of different objects in the image. On highways or urban roads, the road surface is typically paved with black asphalt, and white or yellow lane markings are used to delineate different lanes on the road. Therefore, utilizing edge features in images can effectively extract lane marking information. Edge detection, in essence, involves finding a collection of pixels where significant changes occur, thus extracting the target image composed of these changes. This paper uses an improved Canny algorithm for road lane detection. The traditional Canny algorithm follows the following steps for edge detection:

[1] Image Capture: Since the lane lines to be recognized in this task primarily exhibit straight-line characteristics, images with a resolution of 672 × 37 pixels were captured from the dashcam. These images contain lane lines with straight-line features, making it feasible to employ traditional image processing algorithms for detection.

[2] Image Grayscale Conversion: The original image comprises RGB channels, which can be inconvenient for subsequent traditional image processing operations. Therefore, to facilitate further operations, the image is first converted to grayscale. Since the human eye is most sensitive to green and least sensitive to blue, a weighted average of the *R*, *G*, and *B* components results in a reasonably suitable grayscale image. The grayscale value is calculated using the formula:

$$Gray = 0.114 \cdot B + 0.587 \cdot G + 0.299 \cdot R \tag{5}$$

[3] Image Smoothing: To eliminate noise interference in the image, Gaussian smoothing is applied as the first step. Gaussian filtering is an effective method that uses a Gaussian function to weightedly average pixel values, reducing the influence of noise and making the image smoother [51]. Its formula is shown as 5:

$$G(x, y) = \frac{1}{2\pi\sigma^2} \exp\left(-\frac{x^2 + y^2}{2\sigma^2}\right) \tag{6}$$

Noise reduction is applied to the grayscale lane image, and its effect is shown in the Fig. 4 and Fig. 5.

Figure 4 Original image

Figure 5 Denoised image

[4] Edge Gradient Calculation: Edge gradient direction and magnitude are computed using the finite difference method for each pixel in the image [52]. This is achieved by calculating the gradient values around each pixel, typically using operators such as Sobel and Prewitt, to extract edge information from the image, as shown in Eq. (5):

$$\begin{aligned}
&G(x, y) = \left[C_x^2(x, y) + G_y^2(x, y)\right]^{\frac{1}{2}} \\
&\theta = \arctan\left[\frac{G_x(x, y)}{G_y(x, y)}\right]
\end{aligned} \tag{7}$$

[5] Non-Maximum Suppression: To accurately locate edges, it is necessary to perform non-maximum suppression on the gradient image [53]. This step involves comparing the gradient magnitude of each pixel with its surrounding pixels in the gradient direction, selecting the maximum value, and preserving it to emphasize the edges.

[6] Locating Edges Using Double Threshold Detection. Gradient values are divided into two thresholds: a high threshold and a low threshold. Pixels with gradient values higher than the high threshold are considered strong edge points; those with gradient values between the high and low thresholds are considered weak edge points, while

pixels with values lower than the low threshold are considered background. Then, edges are ultimately located by connecting strong edge points to weak edge points connected to them.

Traditional Canny algorithms using Gaussian filtering can lead to excessive smoothing of the image, reducing useful information. Bilateral filtering, through adaptive weighting, distinguishes between edge and non-edge portions, preserving edge information in the image. It can also retain fine details while smoothing the image. Therefore, replacing Gaussian filtering with bilateral filtering enhances the detection performance, as shown in Eq. (6):

$$g(i,j)\frac{\sum_{(k,l)\in S(i,j)} f(k,l)\,w(i,j,k,l)}{\sum_{(k,l)\in S(i,j)} w(i,j,k,l)} \tag{8}$$

Traditional Canny algorithms compute edge gradient direction and magnitude using the finite difference method, but this method is sensitive to noise. Therefore, this paper introduces an 8-directional Sobel operator to enhance edges and then utilizes the Canny algorithm to extract lane markings. This approach improves edge detection completeness in various environments and exhibits better filtering and edge-preserving capabilities. Edge detection results using the traditional Canny algorithm and the improved Canny algorithm on the same image are shown in Fig. 6 and Fig. 7.

Figure 6 Traditional canny detection result

Figure 7 Results of the proposed algorithm

By comparing Fig. 6 and Fig. 7, The Canny edge detector has a higher edge saliency, resulting in better detection performance.

3.3 System Implementation
3.3.1 System Design

The implementation of the intelligent warning sign adopts K210 as the main controller to control the motor. It is equipped with an onboard camera to perform road detection and recognition. The system utilizes a 4G transparent transmission module to communicate with the mobile app for mode selection and automatic control. The overall system block diagram is shown in Fig. 8.

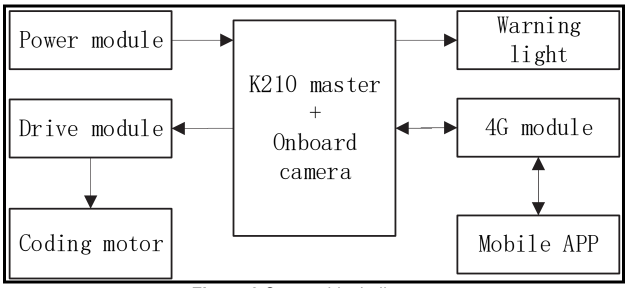

Figure 8 System block diagram

The system mainly consists of three components: hardware modules, software algorithms, and mechanical structure design. The following text will elaborate on the core modules in these three aspects.

3.3.2 Hardware Module Design

[1] K210 Core Module. The SiPEED K210 Core Board, developed by SiPEED, is used as the main controller. The K210 Core Board is an embedded development board based on the RISC-V architecture. It has advantages such as high performance, low power consumption, and low cost [54]. The core schematic diagram is shown in Fig. 9.

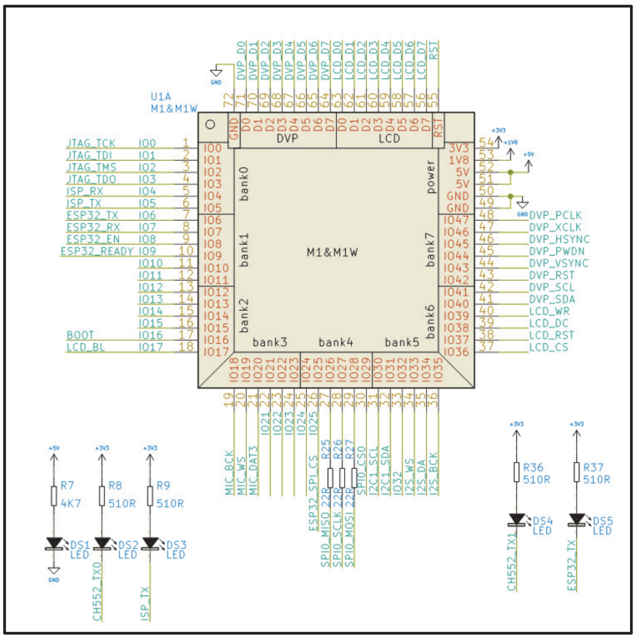

Figure 9 K210 core board schematic diagram

[2] TB6612 Driver Module System Circuit Schematic Diagram. A motor with an encoder is chosen, and speed and control are achieved by adjusting the PWM duty cycle. The TB6612 driver is used to control four motors. The controlled motor voltage range is wide and can operate between 4.5 V and 13.5 V. The TB6612 utilizes an H-bridge structure to distribute current to two motors and controls the direction and speed of the motor based on the control signal [55]. The schematic diagram is shown in Fig. 10.

[3] Camera Module. The built-in camera module of the K210 is used, and Python code is written for road detection. The road detection algorithm is run on the KPU of the K210 to complete road recognition and detection [56]. The camera interface diagram is shown in Fig. 11.

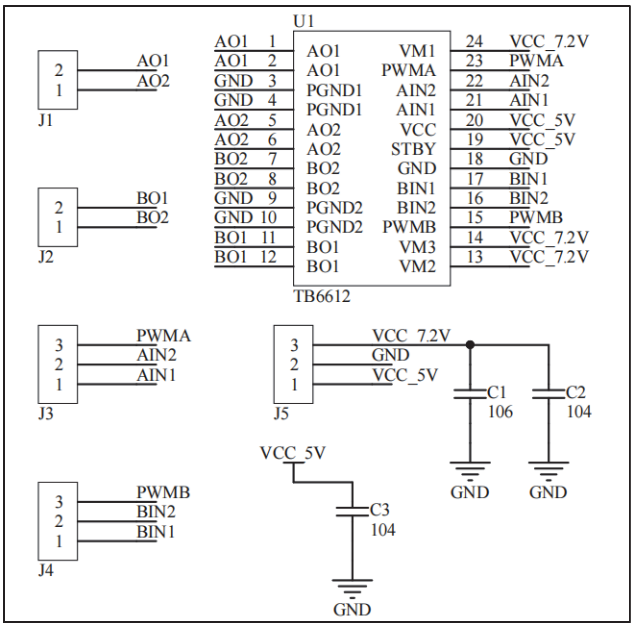

Figure 10 Circuit diagram of the TB6612 drive module

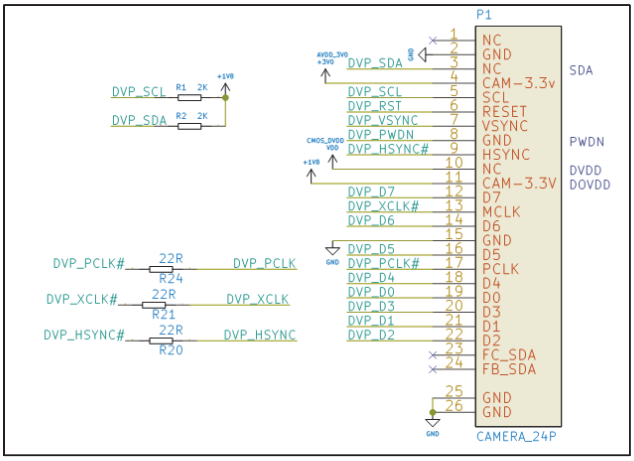

Figure 11 Camera module interface diagram

[4] 4G Wireless Communication Module. The communication between the car and the main controller is a half-duplex communication method. After receiving commands from an Android device, the car responds accordingly. In this system, data interaction between the K210 and the 4G module is achieved through a serial connection using the Air780E model of the 4G module [57]. The control signals are sent from the mobile app to the connected 4G module. The connection method between the K210 main controller and the 4G module is shown in Fig. 12.

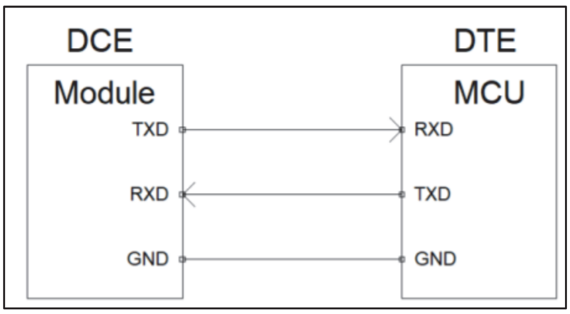

Figure 12 Interface diagram between K210 and Air780E

3.3.3 Mechanical Structure Design

To meet the practical requirements of mobility, foldability, and resilience against external impacts while driving, we have designed a structure that can walk and retract automatically [58]. The 2D plan view of the structure is shown in Fig. 13, while the corresponding 3D structure designed using SolidWorks software is shown in Fig. 14.

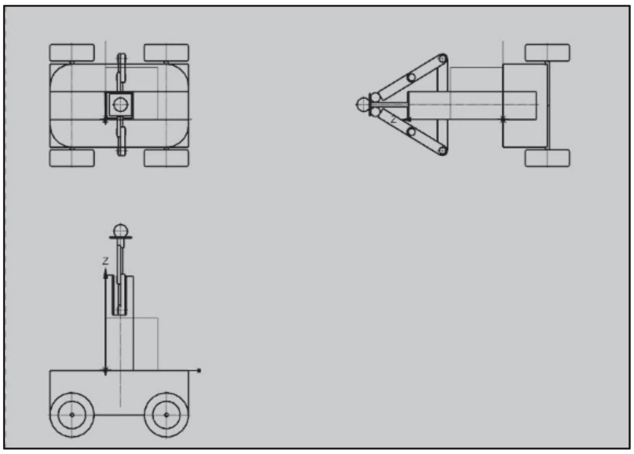
Figure 13 Planar design diagram

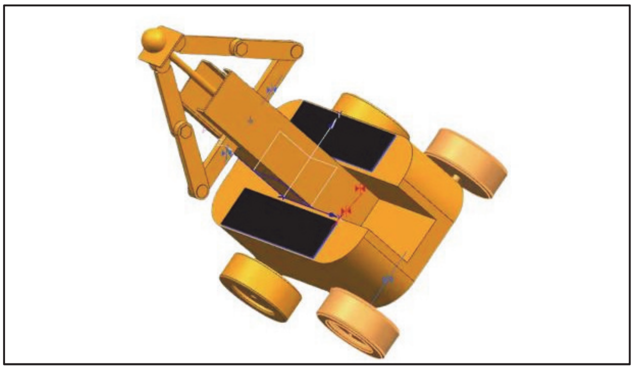
Figure 14 3D structural diagram

3.3.4 Software System Design

[1] Improving the PID Control Algorithm. The system uses the PID algorithm to output pulse width modulation (PWM) signals to control the motor speed. The improved PID algorithm utilizes the real-time speed readings from the encoder and employs an incremental PID algorithm (where the output value is the increment of the control variable). It combines proportional-integral (PI) control in the speed loop to achieve the desired effect of accelerating on straight roads and decelerating on curved roads [59]. The structure is shown in Fig. 15:

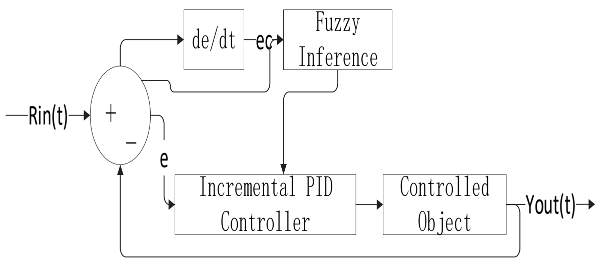

Figure 15 Incremental PID structure diagram

The improved incremental PID control algorithm with good real-time performance can be expressed as follows [60]:

$$\Delta u = k_{p1}\left(e_n - e_{n-1}\right) + k_{p2}\frac{T}{Ti}e_n + \\ +k_{p3}\frac{Td}{T}\left(e_n - 2e_{n-1} + e_{n-2}\right) \tag{8}$$

The PID controller gains k_p, k_i, k_d were empirically tuned to 0.5, 0.2, 0.1 respectively.

The car, while recognizing the white boundary lines on both sides of the road using K210, utilizes the combination of incremental PID and proportional-integral control (the improved PID algorithm) to control the speed loop [61]. This allows for controlling the motor's different speeds to achieve the desired acceleration and deceleration effects for the car.

[2] APP Design. The mobile app is primarily used for mode settings, one-click start, and one-click return functions of the smart warning sign. The app consists of only two interfaces: control interface and settings interface. When the app is launched, the main interface pops up. By clicking the settings button, users can configure the modes in the settings interface, as shown in Fig. 16. Once the settings are completed, users can return to the main interface to control the smart warning sign. The app is designed to be user-friendly with simple operations for user convenience.

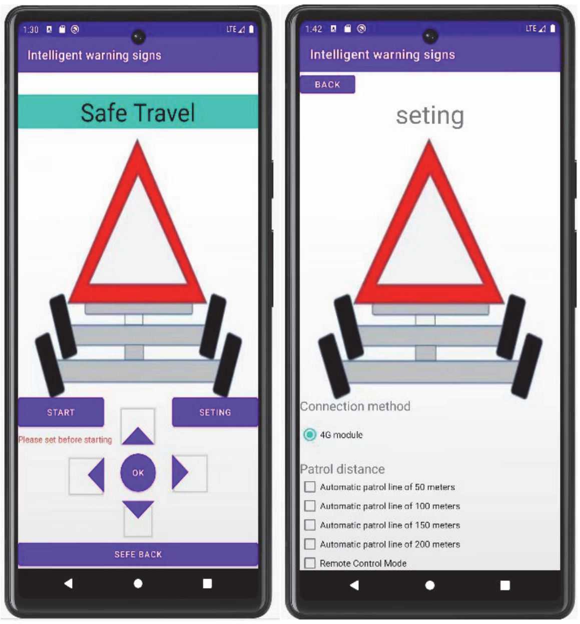

Figure 16 APP display

4 EXPERIMENTALRESULTS AND DISCUSSION

4.1 Evaluation Metrics

In order to compare the performance of different algorithms, this study considers the accurate fitting of detected line segments to the lane lines in the image as a successful detection. On the other hand, the failure of the detection is defined as the inability to accurately fit the detected line segments to the lane lines in the image [62]. The success rate and failure rate are used as evaluation metrics in this experiment, and they are defined as follows:

$$T\left(Success\ Rate\right) = \frac{SD}{NF} \times 100\% \tag{9}$$

$$F\left(Failure\ Rate\right) = \frac{FD}{NF} \times 100\% \tag{10}$$

where SD represents the number of image frames in which the lane lines are accurately fitted, FD represents the number of image frames in which the lane lines are not accurately fitted, and NF represents the total number of image frames.

4.2 Comparative Analysis of Experimental Results

Due to the complex and diverse road conditions in reality, using only a single road condition cannot reflect the performance of the algorithm. Therefore, this article selects multiple test samples to test the algorithm, including various scenarios such as sunny, rainy, day, and night. In order to better extract lane lines, Laplacian or Sobel or Prewitt operators are used for edge enhancement, and then Canny or Hough algorithms are used to extract lane lines. The specific test results for various scenarios are averaged as shown in the Tab. 1.

Table 1 Test result

	T / %	F / %
Laplacian + Canny	71	29
Sobel + Canny	74	26
Prewitt + Canny	68	32
Laplacian + Hough	65	35
Sobel + Hough	69	31
Prewitt + Hough	63	37

According to the test results in the table above, the Sobel + Canny combination excels in image edge detection, achieving an accuracy of 74%. The Sobel operator has excellent gradient calculation performance, and its combination with the Canny edge detector enables effective identification of strong edge structures.

The performance of the Laplacian + Canny combination is slightly below that of Sobel + Canny, but it still demonstrates commendable performance with an accuracy of 71%. The Laplacian operator is used for edge detection, and the Canny edge detector refines the detection of edge structures, contributing to improved accuracy.

The performance of the Prewitt + Canny combination is relatively poorer with an accuracy of 68%. This may be attributed to the Prewitt operator's relatively weaker response to certain edge structures, making it less effective in edge recognition in some cases.

When applying the Hough transform, the Sobel + Hough combination performs the best, achieving an accuracy of 69%. This is likely due to the Sobel operator being more suitable for detecting straight-line edges, and its combination with the Hough transform aids in the effective detection of such edges.

The performance of the Prewitt + Hough combination is the poorest, with an accuracy of 63%. This is possibly due to the Prewitt operator's less stable response and its relatively poor performance in detecting curved edges, which has a detrimental impact in the context of the Hough transform.

A comprehensive analysis leads to the conclusion that the success rate of lane detection with the Canny algorithm is higher than that with the Hough algorithm. Different edge enhancement operators yield varying results, and the highest success rate for lane detection is achieved when using the Sobel operator for edge enhancement. Therefore, this paper first applies the Sobel operator for edge enhancement and then uses the Canny algorithm for lane extraction.

4.3 Multidirectional Sobel Operator

The traditional Sobel operator only considers the horizontal and vertical directions of the image, with less consideration for directional features, which can easily lose some edge details [63]. This article uses the Sobel operator as a model and proposes edge enhancement algorithms for multiple directions, divided into four Sobel operators and eight Sobel operators. The Sobel operators in four directions have added templates in the 45° and 135° directions to the traditional Sobel operator, as shown in Fig. 17.

2	1	0
1	0	-1
0	-1	-2

0	-1	-2
1	0	-1
2	1	0

Figure 17 Sobel operator templates in four directions

The Sobel operators in 8 directions have added templates in 22.5°, 67.5°, 112.5°, and 157° directions to the Sobel operators in 4 directions, and adopt 5 ×. The template for 5 is shown in Fig. 18.

0	0	0	0	0	0	0	0	0	0
-1	-2	-4	-2	-1	0	-2	-4	-2	0
0	0	0	0	0	-1	-4	0	-4	-1
1	2	4	2	1	0	2	4	2	0
0	0	0	0	0	0	0	0	0	0

0	0	0	-1	0	0	0	-1	0	0
0	-2	-4	0	1	0	-2	-4	-2	0
0	-4	0	4	0	0	-4	0	-4	0
-1	0	4	2	0	0	-2	4	2	0
0	1	0	0	0	0	0	1	0	0

0	-1	0	1	0	0	0	1	0	0
0	-2	0	2	0	0	-2	4	2	0
0	-4	0	4	0	0	-4	0	4	0
0	-2	0	2	0	0	-2	-4	2	0
0	-1	0	1	0	0	0	-1	0	0

0	1	0	0	0	0	0	0	0	0
-1	0	4	2	0	0	2	4	2	0
0	-4	0	4	0	-1	-4	0	4	1
0	-2	-4	0	1	0	-2	-4	-2	0
0	0	0	-1	0	0	0	0	0	0

Figure 18 Sobel operator templates for 8 directions

The results of edge enhancement using traditional Sobel operators, 4-direction Sobel operators, and 8-direction Sobel operators are shown in Tab. 2.

Table 2 Different Sobel operator edge enhancements

	Traditional Sobel	Sobel in 4 directions	Sobel in 8 directions
T /	74	78	85
F / %	26	22	15

The traditional Sobel operator has an accuracy of 74% and an error rate of 26%. It can only detect edges in the horizontal and vertical directions, showing weaker responsiveness to slanted or non-horizontal/vertical edges. Therefore, its performance is relatively poor when dealing with edges in multiple directions.

The 4-direction Sobel operator performs better in terms of accuracy, achieving 78%, with an error rate of 22%. This is due to its use of four different directional Sobel kernels, providing a more comprehensive detection of edges at various angles. This enhances the accuracy of edge detection, although it still may not cover all scenarios.

The 8-direction Sobel operator performs the best with an accuracy of 85% and an error rate of 15%. It uses more directions for edge detection, making it better suited for various edge structures. This enables it to excel in the detection of edges in multiple directions.

In summary, the 8-direction Sobel operator performs best in edge enhancement tasks as it comprehensively captures different directional edge structures. While the traditional Sobel operator is simple, its performance is limited when dealing with non-horizontal and non-vertical edges. The 4-direction Sobel operator falls in between, offering moderate accuracy and error rates. Therefore, the choice of the appropriate Sobel operator should depend on specific application requirements and image characteristics, but the 8-direction Sobel operator is typically a more comprehensive and accurate choice, as evidenced by experimental results in this paper.

5 CONCLUSION

The design of an intelligent warning sign based on the improved Canny algorithm aims to address safety and prevention issues following highway vehicle accidents. Compared to traditional lane detection algorithms, the use of multi-directional Sobel edge enhancement and improved Canny-based edge detection offers greater adaptability to various environments and higher performance. Under K210 hardware conditions, this intelligent warning sign exhibits higher precision and speed in lane detection and recognition, effectively reducing the risk of secondary accidents.

Since non-traffic vehicles are currently not permitted on the roads, this study conducted experiments and tests using a simulated lane, providing a solution for the future implementation of intelligent tripods. This product, designed for consideration as a finished product, is primarily controlled by the K210. The K210 can achieve a maximum frame rate of 60FPS, depending on the camera's resolution and sampling rate. In practical use, the frame rate is lower, and real-time performance needs further improvement. Subsequent research may consider switching to a more suitable main controller.

6 REFERENCES

[1] Ding, B. M. (2023). *Radar and Camera Fusion in Intelligent Transportation System*. Doctoral dissertation.

[2] De, B. T., Vaculín, O., & Marzbani, H. (2023). Increasing Safety of Automated Driving by Infrastructure-Based Sensors. *IEEE Access*, *11*, 116781-116793. https://doi.org/10.1109/ACCESS.2023.3311136

[3] Liu, W., Hua, M., & Deng, Z. (2023). A systematic survey of control techniques and applications in connected and automated vehicles. *IEEE Internet of Things Journal*. https://doi.org /10.1109/JIOT.2023.3307002

[4] Li, Z., Yan, T., & Fang, X. (2023). Low-dimensional wide bandgap semiconductors for UV photodetectors. *Nature Reviews Materials*, *9*, 1-17. https://doi.org/10.1038/s41578-023-00583-9

[5] Zhai, L. & Almukhtar, F. H. (2023). A computer vision-based lane detection technique using gradient threshold and hue-lightness-saturation value for an autonomous vehicle. *International Journal of Electrical and Computer Engineering*, *13*(1), 347. https://doi.org /10.11591/ijece.v13i1.pp347-357

[6] Guo, S., Jiang, Y., & Li, J. (2023). Road environment perception for safe and comfortable driving. *Autonomous Driving Perception: Fundamentals and Applications*, 357-387.

[7] Liu, B., Wang, H., & Wang, Y. (2023). Lane Line Type Recognition Based on Improved YOLOv5. *Applied Sciences*, *13*(18), 10537. https://doi.org/10.3390/app131810537

[8] Farid, A., Hussain,F., & Khan, K. (2023). A Fast and Accurate Real-Time Vehicle Detection Method Using Deep Learning for Unconstrained Environments. *Applied Sciences*, *13*(5), 3059. https://doi.org/10.3390/app13053059

[9] Sultana, S. & Ahmed, B. (2023). Vision-Based Robust Lane Detection and Tracking in Challenging Conditions. *IEEE Access*, 11, 82785-82796. https://doi.org /10.1109/ACCESS.2023.3292128

[10] Shashidhar, R., Arunakumari, B. N., & Manjunath, A. S. (2022). Computer Vision and the IoT-Based Intelligent Road Lane Detection System. *Mathematical Problems in Engineering*, *2022*, 4755113. https://doi.org/10.1155/2022/4755113

[11] Syed, M. H., & Kumar, S. (2022). Road Lane Line Detection Based on ROI Using Hough Transform Algorithm. *Advances in Computing and Data Sciences, Springer Nature Singapore*, 567-580.

[12] Stojanović, D., Četić, N., & Kocić, J. (2023). Improving Lane Annotation in Autonomous Driving Data Sets with Classical Computer Vision Techniques*. IEEE*, 1-6. https://doi.org /10.1109/ZINC58345.2023.10174073

[13] Zhang, J. Q., Duan, H. B., & Chen, J. L. (2023). Hough Lane Net: Lane detection with deep Hough transform and dynamic convolution. *Computers & Graphics*, *116*, 82-92. https://doi.org/10.1016/j.cag.2023.08.012

[14] Eepari, V. B., Kumar, T. S. P., & Krishna, P. M. (2023). Road Lane Line Detection.

[15] Li, J. (2023). Lane Detection with Deep Learning: Methods and Datasets. *Information Technology and Control*, *52*(2), 297-308.

[16] Liu, R., Cai, W., & Zhang, J. (2023). CF-lines: a fusing contour features optimization method for line segment detector. *The Journal of Supercomputing*, 1-19.

[17] Cai, W., Liu, R., & Chen, N. (2023). PPL-net: Convolutional Neural Network-Based Polymorphic Points-Line verification framework. *Robotics and Intelligent System*, 89-94. https://doi.org/10.1117/12.2655990

[18] Yin, H., Tian, D., & Lin, C. (2023). V2VFormer $++ $: Multi-Modal Vehicle-to-Vehicle Cooperative Perception via Global-Local Transformer. *IEEE Transactions on Intelligent Transportation Systems.* https://doi.org /10.1109/TITS.2023.3314919

[19] Alaa, M., Salama, G. M., & Galal, A. I. (2022). A Robust Lane Detection Method for Urban roads. *Journal of Advanced Engineering Trends*, *41*(1), 13-26. https://doi.org /10.21608/JAET.2020.37172.1025

[20] Yang, Y., Peng, H., & Li, C. (2022). LaneFormer: Real-Time Lane Exaction and Detection via Transformer. *Applied Sciences*, *12*(19), 9722. https://doi.org/10.3390/app12199722.

[21] Zakaria, N. J. & Shapiai, M. I. (2023). Lane detection in autonomous vehicles: A systematic review. *IEEE Access.* https://doi.org /10.1109/ACCESS.2023.3234442.

[22] Hu, J. (2020). Research on lane detection based on global search of dynamic region of interest (DROI). *Applied Sciences*, 10(7), 2543. https://doi.org/10.3390/app10072543

[23] Yoo, J. H., Lee, S.W., & Park, S. K. (2023). A robust lane detection method based on vanishing point estimation using the relevance of line segments. *IEEE Transactions on Intelligent Transportation Systems*, *18*(12), 3254-3266. https://doi.org /10.1109/TITS.2017.2679222

[24] Bhagwan, P. S. (2023). Study of B Snake based lane detection and tracking Mechanism using Canny Hough Estimation of Vanishing Points algorithm.

[25] Guo, Y., Liu, F., & Ma, Y. (2023). Vanishing point detection of unstructured road based on two-line exhaustive search. *SPIE*, *12509*, 191-200. https://doi.org/10.1117/12.2655990

[26] Feng, Y., Zhou, K., & Li, J. (2023). Incremental Learning-based Lane Detection for Automated Rubber-Tired Gantries in Container Terminal. *IEEE Transactions on Circuits and Systems for Video Technology.* https://doi.org /10.1109/TCSVT.2023.3313576

[27] Yang, J., Guo, S., & Bocus, M. J. (2023). Semantic segmentation for autonomous driving. *Autonomous Driving Perception: Fundamentals and Applications*, *Springer Nature Singapore*, 101-137.

[28] Yu, J., Zhang, J., & Shu, A. (2023). Study of convolutional neural network-based semantic segmentation methods on edge intelligence devices for field agricultural robot navigation line extraction. *Computers and Electronics in Agriculture*, *209*, 107811. https://doi.org/10.1016/j.compag.2023.107811

[29] Pan, X., Shi, J., & Luo, P. (2018). Spatial as deep: Spatial CNN for traffic scene understanding. *Proceedings of the AAAI Conference on Artificial Intelligence*. https://doi.org/10.1609/aaai.v32i1.12301

[30] Wang, J., Wu, Q. M., & Zhang, N. (2023). You Only Look at Once for Real-time and Generic Multi-Task. https://doi.org/10.48550/arXiv.2310.01641

[31] Nguyen, H. (2023). Deep Feature Fusion Network for Lane Line Segmentation in Urban Traffic Scenes. *International Journal of Advanced Computer Science and Applications, 14*(6). https://doi.org /10.14569/IJACSA.2023.0140646

[32] Dong, W., Zhou, L., & Ding, S. (2023). Fast and Intelligent Ice Channel Recognition Based on Row Selection. *Journal of Marine Science and Engineering*, *11*(9),1652. https://doi.org/10.3390/jmse11091652

[33] Xue, Q., Wang, X., & Tu, G. (2023). OTLD: A four-stages visual system for perception of autonomous vehicles. https://doi.org/10.21203/rs.3.rs-3132840/v1

[34] Yoo, S., Lee, H. S., & Myeong, H. (2020). End-to-end lane marker detection via row-wise classification. *Proceedings of the IEEE/CVF conference on computer vision and pattern recognition workshops*,1006-1007.

[35] Yang, Z., Yang, X., & Wu, L. (2022). Pre-Inpainting Convolutional Skip Triple Attention Segmentation Network for AGV Lane Detection in Overexposure Environment. *Applied Sciences*, *12*(20), 10675. https://doi.org/10.3390/app122010675

[36] Wang, S., Nguyen, C., & Liu, J. (2023). Homography Guided Temporal Fusion for Road Line and Marking

Segmentation. *Proceedings of the IEEE/CVF International Conference on Computer Vision*.
[37] Zeng, Y., Meng, W., & Guo, C. (2023). Fast Lane Detection Based on Attention Mechanism. *2023 8th International Conference on Intelligent Computing and Signal Processing (ICSP)*, *IEEE*, 518-522. https://doi.org /10.1109/ICSP58490.2023.10248876
[38] Qin, Z., Wang, H., & Li, X. (2020). Ultra-fast structure-aware deep lane detection. Computer Vision-ECCV 2020: 16th European Conference, Glasgow, UK, August 23-28, 2020, Proceedings, Part XXIV 16. *Springer International Publishing*, 276-291.
[39] Zulkeefli, S. N. (2022). Comparison of CNN-based algorithms for halal logo recognition. *Journal of System and Management Sciences*, *12*(5), 155-168. https://doi.org/10.33168/JSMS.2022.0510
[40] Sarp, S., Kuzlu, M., Zhao, Y., & Cetin, M. (2022). A Comparison of Deep Learning Algorithms on Image Data for Detecting Floodwater on Roadways. *Computer Science and Information Systems*, *19*(1), 397-414. https://doi.org/10.2298/CSIS210313058S
[41] Kim, B. H. (2022). Implementation of access control system based on face prediction and face tracking. *Journal of System and Management Sciences*, *12*(2), 367-377. https://doi.org/10.33168/JSMS.2022.0219
[42] Tabelini, L., Berriel. R., & Paixao, T. M. (2021). Keep your eyes on the lane: Real-time attention-guided lane detection. *Proceedings of the IEEE/CVF conference on computer vision and pattern recognition*.
[43] Feng, Z., Guo,S., & Tan, X. (2022). Rethinking efficient lane detection via curve modelling. *Proceedings of the IEEE/CVF Conference on Computer Vision and Pattern Recognition*. https://doi.org/10.48550/arXiv.2203.02431
[44] Pan, H., Chang, X., & Sun, W. (2023). Multitask Knowledge Distillation Guides End-to-End Lane Detection. *IEEE Transactions on Industrial Informatics.* https://doi.org /10.1109/TII.2023.3233975
[45] He, Y., Chen, W., & Li, C. (2021). Fast and accurate lane detection via graph structure and disentangled representation learning. *Sensors*, *21*(14), 4657. https://doi.org/10.3390/s21144657
[46] Philion, J. (2019). Fastdraw: Addressing the long tail of lane detection by adapting a sequential prediction network. *Proceedings of the IEEE/CVF conference on computer vision and pattern recognition.*
[47] Sato, T. & Chen, Q. A. WIP: On Robustness of Lane Detection Models to Physical-World Adversarial Attacks.
[48] Chaple, G. N. & Daruwala, R. D. (2015). Comparisions of Robert, Prewitt, Sobel operator based edge detection methods for real time uses on FPGA. *2015 International Conference on Technologies for Sustainable Development (ICTSD)*, *IEEE*, *1-4*. https://doi.org /10.1109/ICTSD.2015.7095920
[49] Hou, X. & Ma, Y. (2023). SAR minimum entropy autofocusing based on Prewitt operator. *Plos one*, *18(2)*, *276051*. https://doi.org/10.1371.
[50] Fjortoft, R., Lopes, A., & Marthon, P. (1998). An optimal multiedge detector for SAR image segmentation. *IEEE Transactions on Geoscience and Remote Sensing*, *36*(3), 793-802. https://doi.org /10.1109/36.673672
[51] Gedraite, E. S. (2011). Hadad M. Investigation on the effect of a Gaussian Blur in image filtering and segmentation. *Proceedings ELMAR-2011*, *IEEE*, *393-396.*
[52] Shrivakshan, G. T., & Chandrasekar, C. (2012). A comparison of various edge detection techniques used in image processing. *International Journal of Computer Science Issues (IJCSI)*, *9*(5), 269.
[53] Chen, J. S. & Medioni, G. (1989). Detection, localization, and estimation of edges. *IEEE Transactions on Pattern Analysis and Machine Intelligence*, *11*(2), 191-198. https://doi.org /10.1109/34.16714
[54] Zhou, Z., Ruan, T., & Wang, T. (2021). Design and Research of Non-contact Temperature Measurement and Identity Recognition System. *Journal of Physics: Conference Series*, *IOP Publishing*, *2083*(3), 32042. https://doi.org /10.1088/1742-6596/2083/3/032042
[55] Huang, J. (2017). Development of DC motor drive based on TB6612. *2017 5th International Conference on Frontiers of Manufacturing Science and Measuring Technology (FMSMT 2017)*, *Atlantis Press*, 714-717. https://doi.org /10.2991/fmsmt-17.2017.140
[56] Li, N., Zhao, Y., & Pan, Q. (2021). Illumination-invariant road detection and tracking using LWIR polarization characteristics. *ISPRS Journal of Photogrammetry and Remote Sensing*, *180*, 357-369. https://doi.org/10.1016/j.isprsjprs.2021.08.022
[57] Laaki, H., Miche, Y., & Tammi, K. (2019). Prototyping a digital twin for real time remote control over mobile networks: Application of remote surgery. *IEEE Access*, *7*, 20325-20336. https://doi.org /10.1109/ACCESS.2019.2897018
[58] Zhang, Y., Cai, B., & Liu, Y. (2021). Resilience assessment approach of mechanical structure combining finite element models and dynamic Bayesian networks. *Reliability Engineering & System Safety*, 216. https://doi.org/10.1016/j.ress.2021.108043
[59] Liu, G. F., & Li, H. W. (2017). Design of stepper motor position control system based on DSP. *2017 2nd International Conference on Machinery, Electronics and Control Simulation (MECS 2017)*, *Atlantis Press*. https://doi.org /10.2991/mecs-17.2017.38
[60] Yang, X., Huang, M., & Wu, Y. (2023). Observer-Based PID Control Protocol of Positive Multi-Agent Systems. *Mathematics*, *11*(2), 419. https://doi.org/10.3390/math11020419
[61] Wu, J. & Chen, D. (2019). Trajectory following of a tethered underwater robot with multiple control techniques. *Journal of Offshore Mechanics and Arctic Engineering*, *141*(5), 51104. https://doi.org/10.1115/1.4042533
[62] Yinyue, D. (2011). *A Thesis Submitted in Partial Fulfilment of the Requirements for the Degree of Master of Engineering*. Huazhong University of Science and Technology.
[63] Han, L., Tian, Y., & Qi, Q. (2020). Research on edge detection algorithm based on improved Sobel operator. *MATEC Web of Conferences*, *EDP Sciences*, 309. https://doi.org/10.1051/matecconf/202030903031

Contact information:

Yuan-shuai LAN
(Corresponding author)
School of Electronic Information Engineering,
Greely University of China, Chengdu, Sichuan,
123, Section 2, Chengjian Avenue, Eastern New Area,
Jianyang City, Chengdu City, Sichuan Province
E-mail: 448916030@qq.com

Qian WANG,
School of Electronic Information Engineering,
Greely University of China, Chengdu, Sichuan,
123, Section 2, Chengjian Avenue, Eastern New Area,
Jianyang City, Chengdu City, Sichuan Province

Jing-gui YANG,
School of Electronic Information Engineering,
Greely University of China, Chengdu, Sichuan,
123, Section 2, Chengjian Avenue, Eastern New Area,
Jianyang City, Chengdu City, Sichuan Province

Xue-qin MENG
School of Electronic Information Engineering,
Greely University of China, Chengdu, Sichuan,
123, Section 2, Chengjian Avenue, Eastern New Area,
Jianyang City, Chengdu City, Sichuan Province

Yao YANG
School of Electronic Information Engineering,
Greely University of China, Chengdu, Sichuan,
123, Section 2, Chengjian Avenue, Eastern New Area,
Jianyang City, Chengdu City, Sichuan Province